Journal of Power Sources 218 (2012) 174–180

Contents lists available at SciVerse ScienceDirect

Journal of Power Sources

journal homepage: www.elsevier.com/locate/jpowsour

Impact of isoelectric points of nanopowders in electrolytes on electrochemical characteristics of dye sensitized solar cells

Shyama Prasad Mohanty, Parag Bhargava*

Department of Metallurgical Engineering and Materials Science, Indian Institute of Technology Bombay, Mumbai 400076, India

HIGHLIGHTS

- Different isoelectric point nanopowders were used for preparation of electrolytes.
- Zeta potential measurement confirmed the adsorption of ions on powder surface.
- Cations get adsorbed onto the surface of powders having low isoelectric point.
- Anions were adsorbed on the surface of high isoelectric point powder.
- Electrolyte loaded with high isoelectric point powder shows poor cell performance.

ARTICLE INFO

Article history:
Received 4 April 2012
Received in revised form
13 June 2012
Accepted 17 June 2012
Available online 2 July 2012

Keywords:
Isoelectric point
Zeta potential
Adsorption
Nanopowder loaded electrolyte
Electrochemical
Dye sensitized solar cell

ABSTRACT

Nanoparticle loaded quasi solid electrolytes are important from the view point of developing electrolytes for dye sensitized solar cells (DSSCs) having long term stability. The present work shows the influence of isoelectric point of nanopowders in electrolyte on the photoelectrochemical characteristics of DSSCs. Electrolytes with nanopowders of silica, alumina and magnesia which have widely differing isoelectric points are used in the study. Adsorption of ions from the electrolyte on the nanopowder surface, characterized by zeta potential measurement, show that cations get adsorbed on silica, alumina surface while anions get adsorbed on magnesia surface. The electrochemical characteristics of nanoparticulate loaded electrolytes are examined through cyclic voltammetry (CV) and electrochemical impedance spectroscopy (EIS). DSSCs fabricated using liquid, silica or alumina loaded electrolytes exhibit almost similar performance. But interestingly, the magnesia loaded electrolyte-based cell show lower short circuit current density (J_{SC}) and much higher open circuit voltage (V_{OC}), which is attributed to adsorption of anions. Such anionic adsorption prevents the dark reaction in magnesia loaded electrolyte-based cell and thus, enhances the V_{OC} by almost 100 mV as compared to liquid electrolyte based cell. Also, higher electron life time at the titania/electrolyte interface is observed in magnesia loaded electrolyte-based cell as compared to others.

1. Introduction

Dye sensitized solar cells (DSSCs) are low cost photovoltaics which have attained an efficiency of 12.3% in the lab scale [1]. Most of the higher efficiency DSSCs are based on liquid electrolytes. Liquid electrolytes based cells show the tendency of solvent volatilization over a period of time. Hence, work is being carried out on development of solid electrolyte or quasi solid electrolytes as substitutes for liquid electrolytes. Typically, solid electrolyte based cells are inferior in performance to those based on liquid electrolyte due to improper filling of mesoporous electrode and poor hole mobility [2,3]. In contrast, quasi solid electrolytes achieve almost similar performance as liquid electrolytes with enhanced longevity of the cell [4–6]. These electrolytes have been prepared using 3-D polymer network or contiguous network of nanopowders to achieve gelation of liquid electrolyte [6]. Thermal energy is required to make a homogeneous mixture and trap the liquid in the entangled polymeric network [4]. Alternatively, initiators are required to chemically form the network from monomer units [7]. Gelation process with the use of nanopowders is much simpler as compared to polymers. Addition of nanopowders, beyond a certain weight fraction to liquid electrolytes leads to gel formation. Several nanopowders such as silica, titania, carbon black and carbon nanotubes have been utilized for the purpose [6,8–10]. In case of silica, titania the cationic part of the iodide salt in the electrolyte

* Corresponding author. Tel.: +91 22 25767628; fax: +91 22 25726975.
E-mail address: pbhargava@iitb.ac.in (P. Bhargava).

0378-7753/$ – see front matter © 2012 Elsevier B.V. All rights reserved.
http://dx.doi.org/10.1016/j.jpowsour.2012.06.080

gets adsorbed onto the surface of powders and the anions (iodide/triiodide) are held to the cations by electrostatic force. The anions (iodide/triiodide) form well arranged chains which facilitate the charge transfer by the Grotthuss-like exchange mechanism [9]. So, even if the physical diffusion of ions is retarded in the gel electrolyte, the charge transport is almost comparable to that of liquid electrolyte due to the exchange mechanism. Hence, the performance of the cells fabricated by viscous mass of nanoparticulate gel is comparable to that of liquid electrolyte based cells.

Studies carried out by Bhattacharyya et al. have shown that the adsorption of ions on the powders depends on their surface properties [11]. In their study on electrolytes for lithium ion batteries, higher enhancement in conductivity was observed for silica due to its low point of zero charge as compared to titania and alumina. It is well known that the point of zero charge or isoelectric point in reference to the medium pH determines the surface charge of a powder in a particular liquid medium. Thus, the adsorption of ions from the liquid medium becomes dependent on the isoelectric point. So far in literature no systematic study on nanopowder loaded electrolytes in DSSCs with powders of widely different isoelectric points and their effect on cell performance have been reported. The present work shows the effect of electrolytes loaded with powders of different isoelectric point on performance of dye sensitized solar cells.

2. Experimental

2.1. Materials

Powders having low (~2–3), intermediate (~6–8) and high (~12–13) values of isoelectric points were selected for this study. Silica, alumina and magnesia respectively matched the requirement. Hence, silica, alumina and magnesia nanopowders were used to prepare the nanoparticle loaded electrolytes. Silica -Aerosil 200 (Degussa, specific surface area ~200 $m^2\ g^{-1}$), Alumina- Aeroxide Alu C (Degussa, specific surface area ~100 $m^2\ g^{-1}$), Magnesia (High purity superfine, Cottor International, Mumbai, measured specific surface area ~67.8 $m^2\ g^{-1}$) were the nanopowders used. 1-Methyl-3-propylimidazolium iodide (PMII) (≥98% Aldrich), Iodine (LR, Thomas Baker), 4-tert-Butylpyridine (TBP) (96% Aldrich) and 3-Methoxypropionitrile (MPN) (≥98% Aldrich) were used to prepare the electrolyte. Acetonitrile (Merck, GR) was used for washing the gel. Fluorine-doped tin oxide (FTO) glass substrates (TEC 8, sheet resistance 8–9 Ω $\square^{-1}$, Pilkington), TiO_2 nanopowder (P25, Degussa), Polyethylene glycol (M_w = 600) (PEG 600) (Thomas Baker), $RuL_2(NCS)_2$ (L = 2,2′-bipyridyl-4,4′-dicarboxylic acid) (known as N3 dye) (Dyesol) were used for fabrication of cell.

2.2. Preparation of electrolyte

Liquid electrolyte of composition 0.6 M PMII, 0.1 M iodine and 0.5 M TBP in MPN was prepared by mixing the components. Initial studies showed that the performance of the milled nanopowder loaded electrolyte was better than sonicated nanopowder loaded electrolyte. Nanoparticle loaded electrolytes were thus prepared by adding nanopowders to the liquid electrolyte and milling the mix in order to disperse the particles in the electrolyte medium homogeneously. The solid loading of the powders in electrolyte was chosen to be 5 wt%, 10 wt% and 15wt% for silica, alumina and magnesia respectively. The choice of powder loading was to maintain the overall surface area of the powders in the liquid electrolyte nearly same for all as the ratio of specific surface area in case of silica: alumina: magnesia was almost 3:2:1. Zirconia grinding media of 2–3 mm diameter was added in 1:1 ratio to the mixture of nanopowder and liquid electrolyte and roller milled for 8 h at 90 rpm in order to disperse the powder in the electrolyte. Milling process was particularly essential for preparation of magnesia based electrolyte as the magnesia powder which had the least initial surface area could not trap the liquid electrolyte within the particle network unless ball milled.

2.3. Fabrication of cell

Glass substrates were cleaned with detergent solution followed by cleaning with distilled water and ethanol prior to coating of the TiO_2 slurry. Titania slurry was prepared using TiO_2 nanopowder, PEG 600 and ethanol. The mixture was roller milled for 24 h with zirconia grinding media of 2–3 mm diameter. The slurry was then coated on the substrates by doctor blading. The slurry coated substrates were dried at 40 °C followed by sintering at 450 °C for 1 h. The sintered TiO_2 photoanodes were soaked in 0.3 mM ethanolic solution of N3 dye for 24 h. The photoanodes were then rinsed with ethanol to wash the excess dye. Sputter deposited platinum on FTO glass was used as counter electrode. A 25 micron spacer (SX1170-25PF, Solaronix) was placed on photoanode and electrolyte was added. Counter electrode was placed on top and clamped.

2.4. Characterization

Nanopowders were characterized for size by particle size analyzer (Delsa Nano C, Beckman Coulter). Zeta potential of silica, alumina and magnesia nanoparticles as suspended in solvent (MPN) or electrolyte of composition 39 mM PMII and 6.5 mM iodine in MPN was measured using low concentration flow cell of the instrument (Delsa Nano C). 0.13 wt%, 0.26 wt% and 0.39 wt% of silica, alumina and magnesia respectively were suspended in electrolyte. Surface area of MgO powder was measured by Smart sorb 92/93 (Smart Instruments Co., Mumbai). The nanopowders were also observed by transmission electron microscope (TEM) [Philips CM200].

To examine the adsorption of ionic constituents of PMII from the electrolyte on the nanoparticle surface, the nanoparticles were separated from the electrolyte by centrifuging at 10,000 rpm for 10 min followed by washing with acetonitrile to remove the excess ions. Acetonitrile was used for washing as it has nearly same dielectric constant as MPN but its viscosity is lower. The washed gel was dried and the mass obtained was treated as residue of corresponding gel. Thermal analysis was done in flowing air by SDT Q600 (TA Instruments) at a heating rate of 10 °C min^{-1}. FT–IR spectra of samples were recorded using an FTIR spectrophotometer (Jasco 6100). Electrochemical characterization of the electrolyte was done by using PGSTAT (AUTOLAB 302N). A symmetric cell [9] was constructed for this purpose using two sputtered Pt-FTO glass and electrolyte was sandwiched in between them using a 60 μm thick spacer enclosing an area of 1 cm^2 (Fig. 1). Cyclic voltammetry (CV) of the symmetric cell was performed at a scan rate of 10 mV s^{-1} from −1 to+1 V. Impedance measurements were recorded over frequency range from 0.1 MHz to 0.1 Hz with an amplitude of 10 mV.

Photocurrent–voltage (I–V) characteristics were obtained using a Keithley model 2420 source measure unit. The irradiation source was a 150 W xenon lamp on a Newport solar simulator with AM

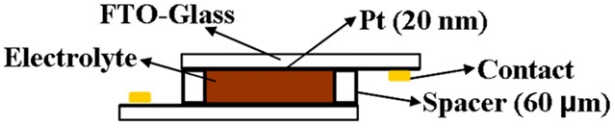

Fig. 1. Schematic of the symmetric cell.

1.5 G. The cell active area was 1 cm^2. Dye loading was determined by desorption of the adsorbed dye with 1 N NaOH solution and comparing with a calibrated curve in UV–visible spectrometer (Jasco V650). Impedance measurements of the cells were recorded over frequency range from 0.1 MHz to 0.1 Hz with an amplitude of 10 mV at open circuit potential.

3. Results and discussion

3.1. Powder characteristics

The average particle sizes as determined by light scattering for silica, alumina and magnesia in suspension were 205 nm, 286 nm and 1282 nm respectively. The specific surface area of magnesia nanopowders was found to be 67.8 $m^2\ g^{-1}$. The particle sizes as calculated from specific surface area were 11 nm, 15 nm and 25 nm for silica, alumina and magnesia respectively. The difference in particle size of the powders determined from specific surface area measurement and light scattering indicated agglomeration. Also, TEM images of silica, alumina and magnesia nanopowders shown in Fig. 2 confirmed that the powders were highly agglomerated. The particle size of silica and alumina as seen in TEM was found to be in between 10 and 15 nm and that of magnesia was found to be >25 nm. Hence, particle size observed under TEM closely matched with that determined using specific surface area.

3.2. Thermal analysis

Thermal analysis of the nanopowders, gel residue samples and PMII respectively are shown in Fig. 3. Differential scanning calorimetry (DSC) of PMII showed an endothermic peak at 315 °C which was associated with the decomposition of PMII. Accompanying thermogravimetric analysis (TGA) showed that PMII decomposes fully leaving no residue. TGA of pure silica powder showed a weight loss of ~2.5% upto 800 °C. The weight loss continued upto high temperature which can be attributed to the chemically bonded water in form of silanol groups. Although the same trend was observed for silica gel residue but the weight loss of additional 2.6% was observed. Similarly, additional 2.3% weight loss was observed in the case of alumina gel residue sample over that of pure alumina powder. While in case of magnesia gel residue although a sharp decrease in mass was observed in the range of PMII decomposition, it was not due to PMII but due to the adsorbed water confirmed by comparing with DSC-TG of pure magnesia powder. Additional weight loss of 1% in magnesia gel residue over that of pure magnesia was observed in TG. The additional weight losses observed in gel residues might be due to negligible amount of adsorbed solvent or PMII or hydration of powders. The initial weight loss below 200 °C was due to the adsorbed moisture in the gel residues.

3.3. FTIR analysis

To further examine the adsorption of PMII on the nanopowders the bonding characteristics were examined from the FTIR measurements. Fig. 4 shows the FTIR spectra of PMII, silica gel residue, alumina gel residue and magnesia gel residue. Additional peaks corresponding to bonding of PMII with the nanopowders were not found in case of silica, alumina and magnesia gel residues when compared with silica, alumina and magnesia nanopowders respectively. So, it indicates the absence of any ions on the surface of nanopowders. Ions are almost completely removed on washing. But the intensity of peak corresponding to presence of hydroxyl group (~3200–3600 cm^{-1}) increased in the residue as compared to corresponding nanopowder. It correlates well with the TG plots where additional weight losses in the residue samples were observed as compared to pure nanopowders at higher temperature. So, the surface of the nanopowders is hydrated owing to exposure to electrolyte as well as the process of washing the gels.

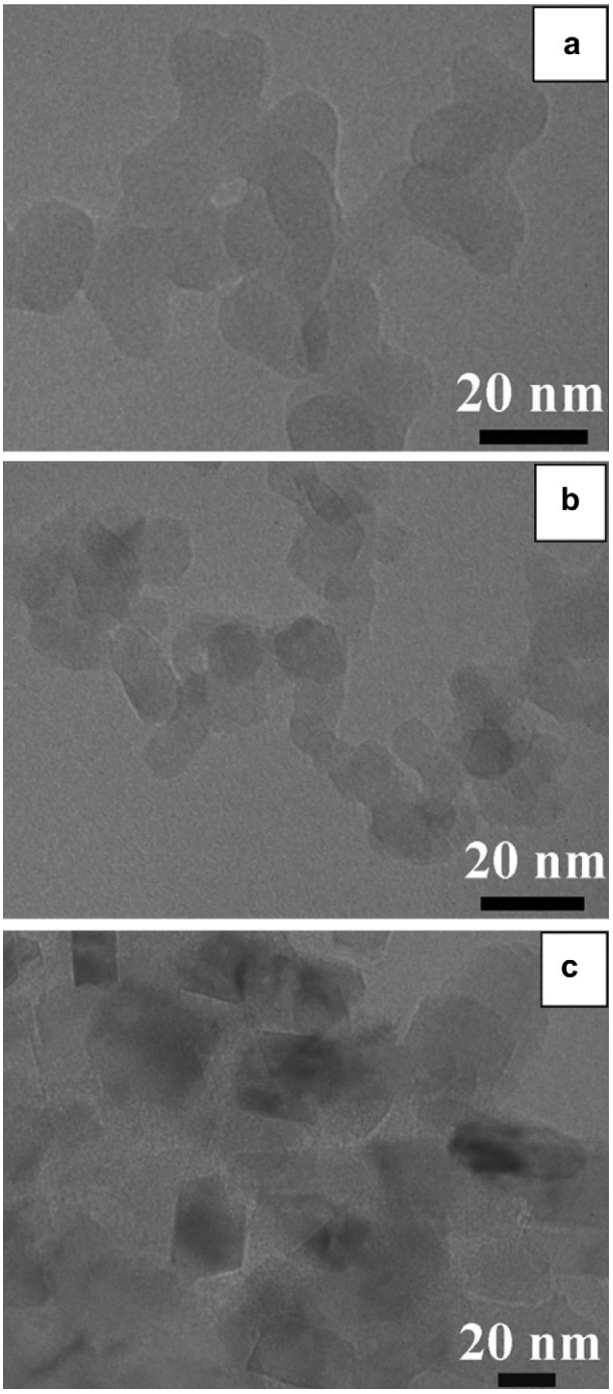

Fig. 2. TEM images of a) Silica, b) Alumina and c) Magnesia.

3.4. Zeta potential measurement

In order to further characterize the interaction of nanopowders with the electrolyte zeta potential was measured. Zeta potential measurement was carried out to observe the surface charge of nanopowders in solvent (MPN) and electrolyte (PMII, I_2 in MPN).

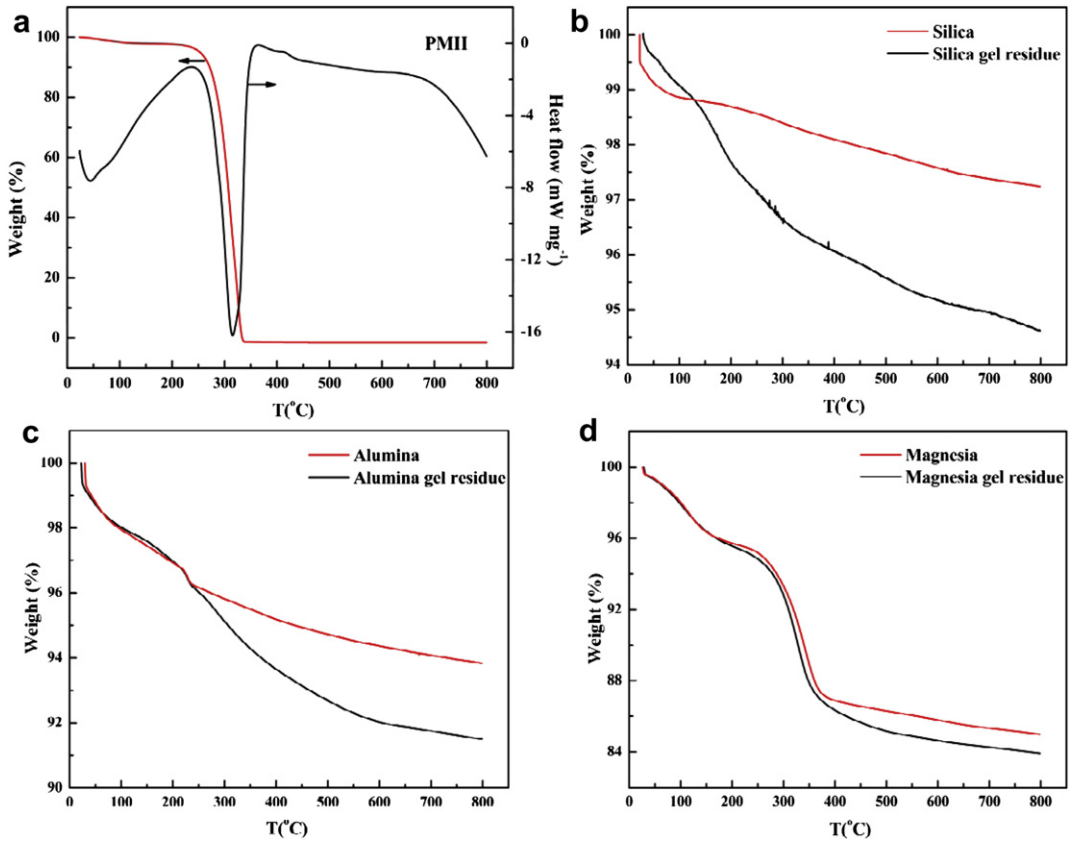

Fig. 3. DSC-TG curves of a) PMII b) silica and silica gel residue c) alumina and alumina gel residue and d) magnesia and magnesia gel residue.

The pH of the solvent and electrolyte was ~6–7. So, as expected silica showed negative zeta potential in solvent (Table 1). But in the electrolyte in presence of PMII and iodine in solvent the zeta potential value for silica changed near to zero indicating adsorption of cationic part of PMII on the silica surface. In case of alumina, similar change was observed but the zeta potential changed from being negative in the solvent to little more positive in the electrolyte. While magnesia was highly positive in the solvent, its value changed to a lower positive value in electrolyte suggesting excess adsorption of negatively charged species. It is thus likely that while cations may be adsorbed on MgO surface as well but relatively larger amount of anionic species (iodide, triiodide) were adsorbed on MgO powder surface. Based on the above observations the probable arrangement of ionic species on nanoparticles in electrolyte is shown in Fig. 5. The results obtained from TGA, FTIR and zeta potential measurements altogether confirmed that ion adsorption only occurred in the electrolyte medium. On washing the gel the ions were completely removed indicating the absence of any chemical bonding between the ionic species and nanoparticles. Thus, the ions were arranged by electrostatic force on the surface of powders.

3.5. Electrochemical analysis of electrolyte

Grotthuss-like mechanism of charge transport occurs in electrolyte by adsorption of imidazolium group ions and corresponding arrangement of iodide/triiodide on the surface of nanopowders [9]. This enhances the charge transport by electron hopping (exchange) even though the physical ion diffusion is retarded by loading of the nanopowders in the liquid electrolyte. So, the net charge transport is comparable to that in the liquid electrolyte. The charge transport may be affected with use of nanopowders in electrolytes that do not allow imidazolium cations to adsorb on powder surface. Fig. 6 shows the electrochemical characteristics of all three-silica, alumina and magnesia nanoparticle loaded electrolytes. In a cyclic voltammogram, the slope indicates resistance offered by the electrolyte towards charge transport. In magnesia the charge transport was slowest as compared to silica or alumina loaded electrolyte as shown by the slope of CV. Small decrease in limiting current density (J_{Lim}) was observed on moving from silica to magnesia while alumina lay in between the two. But the charge transfer resistance (R_{CT}) and iodide/triiodide diffusion resistance (R_{Diff}) were maximum in magnesia. The series resistance (R_S) was lowest for liquid electrolyte due to better fluidity while the adsorption of ions from the electrolyte onto nanopowders surface increases R_S in nanopowder loaded electrolytes. These observations demonstrated the role played by the surface characteristics or isoelectric point of powders in charge transport.

3.6. Current–voltage characteristics

The photovoltaic performance of the DSSCs diminished on moving from silica containing electrolyte to magnesia containing electrolyte as shown in Table 2 and Fig. 7a. Alumina loaded electrolyte showed performance close to silica loaded electrolyte. Despite the difference in isoelectric point, both silica and alumina promoted the adsorption of cationic species. Difference observed in performance of MgO nanoparticulate loaded electrolyte based DSSC is due to the adsorption of anionic species which is confirmed from zeta potential measurements. The slope of CV curves were nearly same for liquid, silica and alumina loaded electrolytes confirming faster charge transport as compared to magnesia loaded

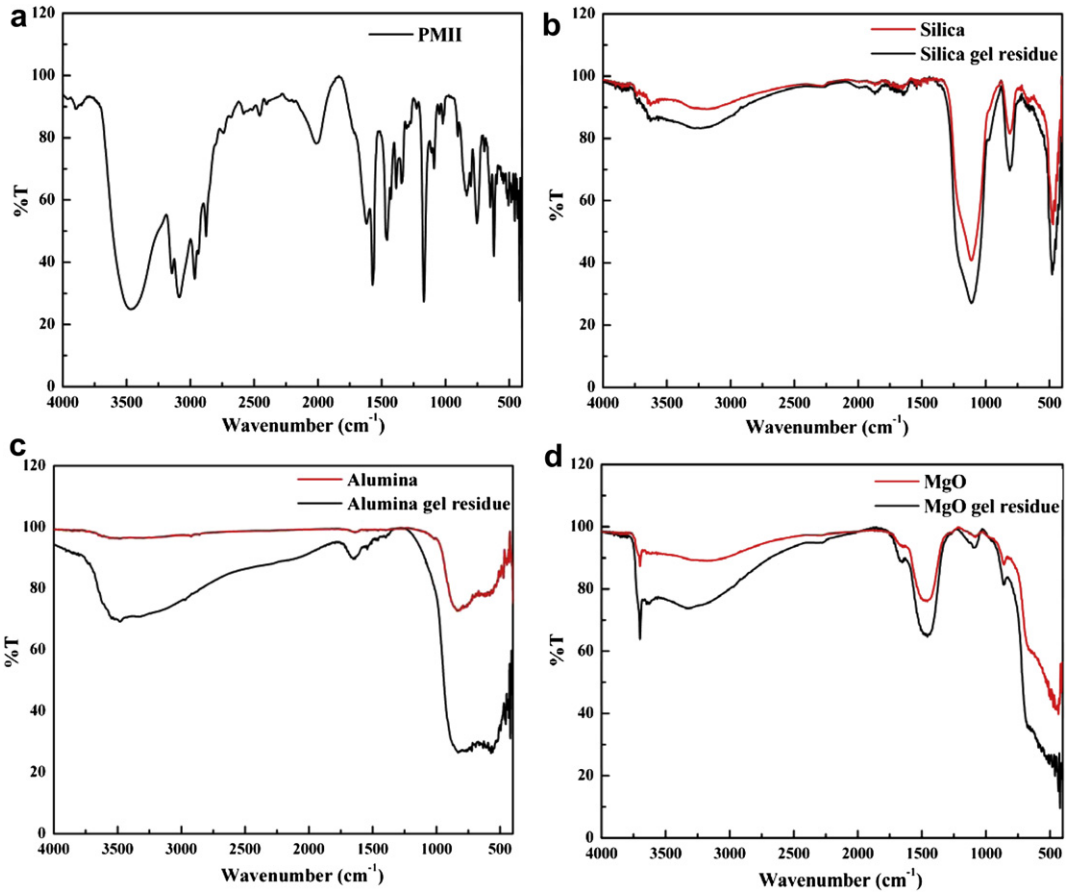

Fig. 4. FTIR spectra of a) PMII b) silica and silica gel residue c) alumina and alumina gel residue d) magnesia and magnesia gel residue.

electrolytes. The higher J_{SC} in silica or alumina loaded electrolytes indirectly supports the Grotthuss-like exchange mechanism as ions are immobilized yet the current is maintained. Even though the dye loading was almost same for all the cells, J_{SC} for magnesia loaded electrolytes based cell was lower than others. This is due to the anionic adsorption (iodide/triiodide on MgO), which caused poor charge transport in the magnesia loaded electrolyte. Dye regeneration is retarded in MgO nanoparticle loaded electrolyte based DSSC as iodide/triiodide redox couple is adsorbed on the MgO surface. Hence, lower photocurrent was obtained in magnesia based electrolyte compared to silica or alumina loaded electrolytes. But interestingly higher V_{OC} was obtained in magnesia based electrolytes which was ascribed to suppressed recombination

Table 1
Zeta potential of nanopowders in solvent and electrolyte.

Sample	Zeta potential (mV)
Silica-MPN	−48.24
Silica-Electrolyte	−1.83
Alumina-MPN	−15.13
Alumina- Electrolyte	8.83
Magnesia-MPN	34.68
Magnesia-Electrolyte	23.15

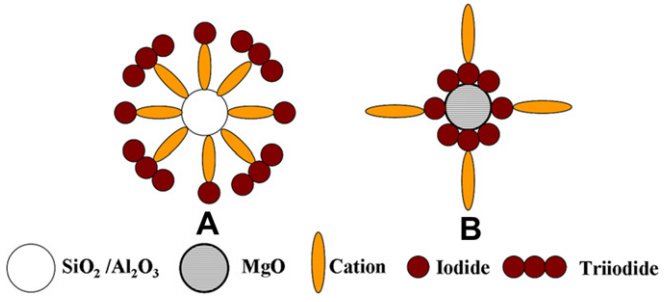

Fig. 5. Probable structure of ions surrounded nanoparticles in the electrolyte A) silica/alumina and B) magnesia.

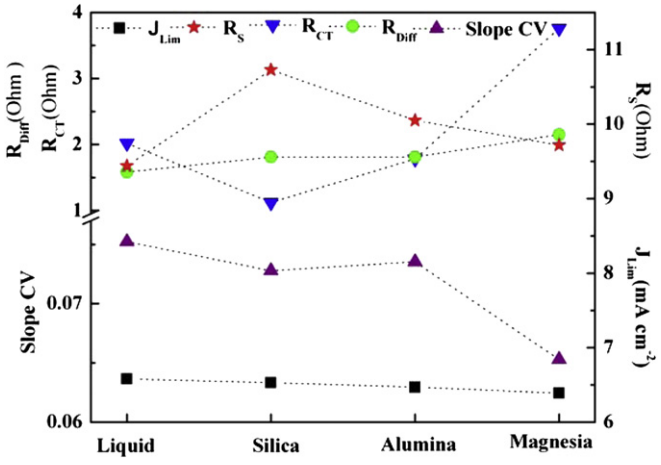

Fig. 6. Electrochemical characteristics of different electrolytes.

Table 2
Effect of different nanopowders on cell performance.

Electrolyte	Dye loading (mol cm^{-2})	J_{SC} (mA cm^{-2})	V_{OC} (mV)	FF (%)	η (%)
Liquid	6.4×10^{-8}	6.6	715	62.5	2.98
5 Wt% Silica	6.6×10^{-8}	6.8	695	64.2	3.04
10 Wt% Alumina	5.8×10^{-8}	6.4	736	64.9	3.07
15 Wt% Magnesia	6.2×10^{-8}	2.3	817	72.9	1.37

reactions at TiO_2/electrolyte interface. Adsorption of triiodide on MgO inhibited recombination of triiodide with the electrons from titania. Lower dark current in case of magnesia loaded electrolyte based cell was also evident to less recombination at the TiO_2/electrolyte interface (Fig. 7b). The origin of higher V_{OC} was also supported by independent observations on open circuit voltage decay measurements. Slowest decay was observed for MgO loaded electrolyte further confirming that the recombination reaction is retarded on addition of MgO to liquid electrolyte. The enhancement in fill factor observed for magnesia loaded electrolytes is due to the reduction in recombination reaction. The shunt resistance of cell depends on the recombination reactions. Reduction in recombination increases the shunt resistance and thus, increases the fill factor of the cell.

3.7. Electrochemical impedance spectroscopic analysis of cells

The photoelectrochemical analysis of the cells showed two distinct semicircles (Fig. 8a). The semicircle at higher frequency (1–10 kHz) corresponds to the charge transfer resistance at the Pt/electrolyte interface. The second semicircle (10–100 Hz) corresponds to the charge transfer resistance at the titania/electrolyte interface. The intercept on *X*-axis by first semicircle corresponds to the series resistance of the cell. As observed from Fig. 8a series resistance of the cell with silica loaded electrolyte was minimum. This essentially was due to better charge transport between the dye adsorbed titania surface and counter electrode because all other components except electrolyte remained same for all the DSSCs. Magnesia loaded electrolyte having slowest charge transport through the electrolyte showed highest series resistance. In addition, the charge transfer resistance at the TiO_2/electrolyte interface was found to be largest for magnesia loaded electrolyte based cell. The characteristic peak frequency (f) corresponding to second semicircle is related to the electron life time (τ_e) by the following equation [12]:

$$\Gamma_e = (2\pi f)^{-1} \quad (1)$$

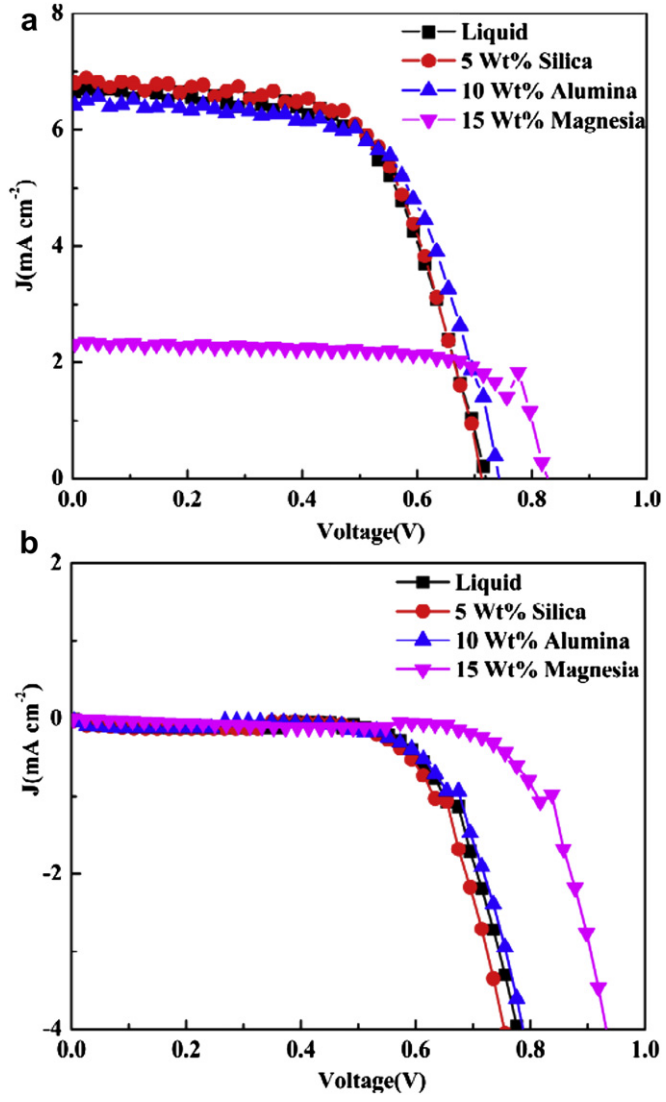

Fig. 7. J–V characteristics of DSSCs with different electrolytes in a) light and b) dark.

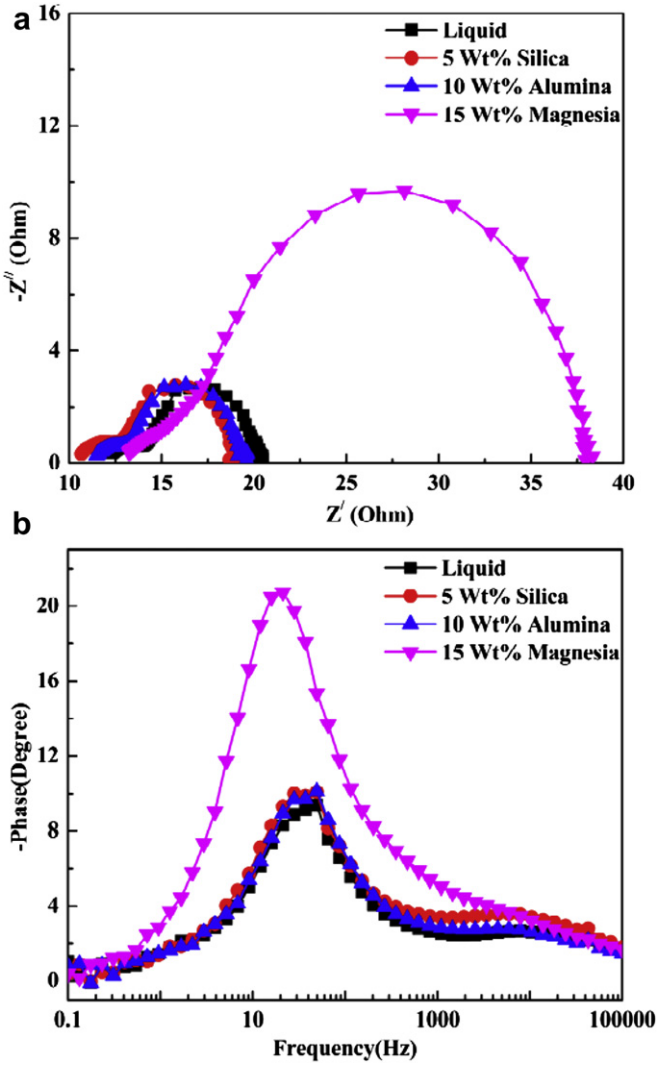

Fig. 8. a) Nyquist plots and b) bode phase plots for dye sensitized solar cells based on different electrolytes.

Peak in case of magnesia loaded electrolyte was shifted to a lower frequency as observed from bode phase plots (Fig. 8b). The electron life time calculated by equation (1) was found to be 13.2 ms for MgO loaded electrolyte based cell while that for liquid and silica or alumina loaded electrolyte was determined to be 5.7 ms. Greater electron life time in case of MgO loaded electrolyte again confirms less recombination at TiO_2/electrolyte interface.

4. Conclusions

The effect of addition of nanopowders with different isoelectric points to the electrolyte on photovoltaic performance of DSSCs was examined. Silica and alumina loaded electrolyte based cells performed almost similar to liquid electrolyte based cell. But addition of magnesia to electrolyte decreased the photocurrent and efficiency of the cells. Adsorption of anionic species (iodide/triiodide) on the nanopowder surface was responsible for poor performance in magnesia based electrolytes. However, photovoltage was enhanced in magnesia based electrolytes due to prevention of recombination reactions. Finally, it was observed that low isoelectric point materials are suitable for nanoparticulate loaded electrolytes which can perform efficiently.

Acknowledgements

The authors acknowledge Corning Inc. USA and DST India (Project code-10DST030) for financial support and Sophisticated Analytical Instruments Facility (SAIF), IIT Bombay for TEM facility. We also thank Evonik Industries, India for providing silica and alumina nanopowders for the study.

References

[1] A. Yella, H.W. Lee, H.N. Tsao, C. Yi, A.K. Chandiran, M.K. Nazeeruddin, E.W.G. Diau, C.Y. Yeh, S.M. Zakeeruddin, M. Grätzel, Science 334 (2011) 629.
[2] D. Li, D. Qin, M. Deng, Y. Luo, Q. Meng, Energy Environ. Sci. 2 (2009) 283.
[3] J.H. Yum, P. Chen, M. Grätzel, M.K. Nazeeruddin, ChemSusChem 1 (2008) 699.
[4] P. Wang, S.M. Zakeeruddin, J.E. Moser, M.K. Nazeeruddin, T. Sekiguchi, M. Grätzel, Nat. Mater. 2 (2003) 402.
[5] J.H. Wu, S.C. Hao, Z. Lan, J.M. Lin, M.L. Huang, Y.F. Huang, L.Q. Fang, S. Yin, T. Sato, Adv. Funct. Mater. 17 (2007) 2645.
[6] P. Wang, S.M. Zakeeruddin, M. Grätzel, J. Fluorine Chem. 125 (2004) 1241.
[7] Z. Lan, J. Wu, J. Lin, M. Huang, S. Yin, T. Sato, Electrochim. Acta 52 (2007) 6673.
[8] P. Wang, S.M. Zakeeruddin, P. Comte, I. Exnar, M. Grätzel, J. Am. Chem. Soc. 125 (2003) 1166.
[9] M. Berginc, M. Hocevar, U.O. Krasovec, A. Hinsch, R. Sastrawan, M. Topic, Thin Solid Films 516 (2008) 4645.
[10] H. Usui, H. Matsui, N. Tanabe, S. Yanagida, J. Photochem. Photobiol. A 164 (2004) 97.
[11] A.J. Bhattacharyya, J. Maier, Adv. Mater. 16 (2004) 811.
[12] R. Kern, R. Sastrawan, J. Ferber, R. Stangl, J. Luther, Electrochim. Acta 47 (2002) 4213.